Electronic Supplementary Information for:

Putting Chromium on the Map for N_2 Reduction: Production of Hydrazine and Ammonia. A Study of *cis*-$M(N_2)_2$ (M= Cr, Mo, W) Bis(diphosphine) Complexes

Jonathan D. Egbert,[‡] Molly O'Hagan,[‡] Eric S. Wiedner,[‡] R. Morris Bullock,[‡] Nicholas A. Piro,[†] W. Scott Kassel,[†] and Michael T. Mock[‡]*

[‡]Center for Molecular Electrocatalysis, Physical Sciences Division, Pacific Northwest National Laboratory, Richland, Washington 99352, United States

[†]Department of Chemistry, Villanova University, Villanova, Pennsylvania 19085, United States

Table of Contents

General Procedures

All synthetic procedures were performed under an atmosphere of N_2 using standard Schlenk or glovebox techniques. Unless described otherwise, all reagents were purchased from commercial sources and were used as received. Protio solvents were dried by passage through activated alumina columns in an Innovative Technology, Inc., PureSolv solvent purification system and stored under N_2 or argon until use. THF-d_8 and benzene-d_6 were purchased from Cambridge Isotope Laboratories and dried over NaK and vacuum transferred before use. Isotopically labelled $^{15}N_2$ was purchased from Cambridge Isotope Laboratories. Magnesium powder, triflic acid, and 1,3,5-trimethoxybenzene were purchased from Sigma-Aldrich and used as received. $CrCl_3(THF)_3$ was purchased from Strem Chemicals Inc. $MoBr_3(THF)_3$,[1] $WCl_4(PPh_3)_2$,[2] and the diphosphine ligand $P^{Et}N^{2,6\text{-}F2\text{-}Bn}P^{Et}$,[3] were prepared by following literature procedures. The ^1H NMR spectra were collected in thin walled NMR tubes on a Varian NMR S 300 or 500 MHz spectrometer. ^1H and ^{13}C NMR chemical shifts are referenced to TMS using the residual protio solvent resonances in the deuterated solvent. ^{31}P chemical shifts are proton decoupled unless otherwise noted and referenced to H_3PO_4 as an external reference. ^{15}N NMR chemical shifts were externally referenced to CH_3NO_2 (δ = 0). Infrared spectra were recorded on a Thermo Scientific Nicolet iS10 FT-IR spectrometer at ambient temperature and under a purge stream of nitrogen gas. Cyclic voltammetry was performed in a Vacuum Atmospheres Nexus II glovebox under an N_2 atmosphere using a CH Instruments model 620D or 660C potentiostat. Measurements were performed using standard three-electrode cell containing a 1 mm PEEK-encased glassy carbon working electrode, Cypress Systems EE040, a 3 mm glassy carbon rod (Alfa) as the counter electrode, and a silver wire suspended in electrolyte solution and separated from the analyte solution by a Vycor frit (CH Instruments 112) as the pseudo-reference electrode

in THF with 0.20 M $[Bu_4N][B(C_6F_5)_4]$ as the supporting electrolyte. Prior to the acquisition of each voltammogram, the working electrode was polished using 0.1μm γ-alumina (BAS CF-1050), and rinsed with THF. Ferrocene or decamethylferrocene was used as an internal reference, and all potentials are reported versus the ferrocenium/ferrocene couple at 0.0 V. Elemental analysis was performed by Atlantic Microlabs, Norcross, GA.

Synthesis of the dinitrogen complexes 1-3

cis-$[Cr(N_2)_2(P^{Et}N^{2,6\text{-}F2\text{-}Bn}P^{Et})_2]$ (**1**): $P^{Et}N^{2,6\text{-}F2\text{-}Bn}P^{Et}$ (0.71 g, 2.0 mmol) was dissolved in ~2 mL of THF and added to a purple solution of $CrCl_3(THF)_3$ (0.38 g, 1.0 mmol) in ~ 50 mL THF that was cooled to -5 °C, resulting in a dark blue solution. After the reaction was stirred for 2 h at -5 °C excess magnesium powder (1.7 g, 70 mmol) was added to the reaction mixture. The reaction was stirred at -5 °C and was periodically monitored for 72 h by ^{31}P NMR for the formation of **1**. After 24 h, ^{31}P NMR analysis showed the formation of **1** but a significant amount of free PNP ligand was also present. After stirring for 72 h the reaction mixture was filtered through a plug of alumina (2 in x ½ in) and the volume of the clear orange solution was reduced to 3 mL under reduced pressure. Cold pentane (stored at -5 °C) (~10 mL) was added to precipitate an orange solid that was collected by filtration and washed with cold pentane to remove unreacted $P^{Et}N^{2,6\text{-}F2\text{-}Bn}P^{Et}$ ligand. The yellow-orange solid was dried briefly under reduced pressure. Yield: 0.031 g (0.039 mmol, 4%). ^1H NMR (500 MHz, THF-d_8, 298 K): δ 7.33 (m, 2H, Ar*H*), 6.97 (m, 4H, Ar*H*), 3.62 (s, 4H, NCH_2Ar), 3.3 (m, 2H, PCH_2N), 3.2 (m, 2H, PCH_2N), 2.38 (m, 2H, PCH_2N), 2.31 (m, 4H, PCH_2CH_3), 2.20 (m, 2H, PCH_2N), 1.89 (m, 2H, PCH_2CH_3), 1.69 (m, 2H, PCH_2CH_3), 1.48 (m, 2H, PCH_2CH_3), 1.41 (m, 4H, PCH_2CH_3), 1.16 (m, 2H, PCH_2CH_3), 0.89-1.10 (m, 24H, PCH_2CH_3). $^{13}C\{^1H\}$ NMR (125.7 MHz, THF-d_8, 298 K): δ 163.2 (m, Ar*C*F, $^1J_{CF}$ = 251 Hz), 130.7 (m, Ar*C*, $^1J_{CF}$ = 167 Hz, $^3J_{CF}$ = 11 Hz), 114.8 (m, Ar*C*), 111.9 (m, Ar*C*, $^1J_{CF}$ =

165 Hz), 58 (m, N*C*H_2P), 54 (m, N*C*H_2Ar), 17-30 (m, P*C*H_2CH$_3$), 6-11 (m, PCH$_2$*C*H$_3$). ^{31}P{^{1}H} NMR (202.4 MHz, THF-d_8, 298 K): δ 37.9 (dd, 2P, $^2J_{PP}$ = 23.4, 27.9 Hz), 32.2 (dd, 2P, $^2J_{PP}$ = 23.4, 27.9 Hz). ^{19}F NMR (470.5 MHz, THF-d_8, 298 K): δ -116.7 (m, 4F). ^{15}N{^{1}H} NMR (50.7 MHz, THF-d_8, 298 K): δ -7.3 (d, 2N, Cr-N≡*N*, $^1J_{NN}$ = 7 Hz), -11.5 (dm, 2N, Cr-*N*≡N, $^1J_{NN}$ = 7 Hz). IR (THF): ν_{NN} cm^{-1} = 1990, 1911. Anal. Calcd. for $C_{34}H_{58}CrF_4N_6P_4$: C, 50.9; H, 7.3; N, 10.5. Found: C, 50.5; H, 7.3; N, 9.95. Complex **1** is remarkably stable in THF at 40 °C for up to three days with a small amount of free PNP ligand being detected in solution after this time. Heating slowly converts **1** to *trans*-**1**, and after 3 days ~20% is converted to the trans isomer.

trans-[Cr(N$_2$)$_2$(P^{Et}N$^{2,6\text{-F2-Bn}}$P^{Et})$_2$] (*trans*-**1**): Following the synthesis of complex **1**, the material removed in the pentane wash performed in the final purification step slowly precipitates a small quantity of *trans*-**1**, a yellow solid. This material was identified as *trans*-**1** by NMR and IR spectroscopies, and X-ray diffraction analysis (see Fig. S1). ^{1}H NMR (500 MHz, THF-d_8, 298 K): δ 7.33 (m, 2H, Ar*H*), 6.97 (m, 4H, Ar*H*), 3.64 (s, 4H, NCH_2Ar), 2.82 (s, 8H, PCH_2N), 1.83 (m, 16H, PCH_2CH$_3$), 1.02 (m, 24H, PCH$_2$CH_3). ^{31}P{^{1}H} NMR (202.4 MHz, THF-d_8, 298 K): δ 37.1 (s, 4P). ^{19}F NMR (470.5 MHz, THF-d_8, 298 K): δ -116.5 (m, 4F). ^{15}N{^{1}H} NMR (50.7 MHz, THF-d_8, 298 K): δ -22.6 (dm, 2N, Cr-*N*≡N, $^1J_{NN}$ = 6 Hz), -28.0 (d, 2N, Cr-N≡*N*, $^1J_{NN}$ = 6 Hz). IR (THF): ν_{NN} cm^{-1} = 1906.

cis-[Mo(N$_2$)$_2$(P^{Et}N$^{2,6\text{-F2-Bn}}$P^{Et})$_2$] (**2**): P^{Et}N$^{2,6\text{-F2-Bn}}$P^{Et} (0.43 g 1.2 mmol) was dissolved in ~2 mL of THF and added to a solution of MoBr$_3$(THF)$_3$ (0.34 g, 0.62 mmol) in ~ 50 mL THF that was cooled to -5 °C, resulting in a blue solution. After the reaction mixture was stirred for 17 h at -5 °C and after this time magnesium powder (1.5 g, 62 mmol) was added to the reaction mixture.

The reaction was stirred at -5 °C and was periodically monitored by ^{31}P NMR for the formation of **2**. After stirring for 8 h, ^{31}P NMR indicated that the free PNP ligand was consumed and **2** was the only observable product in solution. The yellow reaction mixture was filtered through a plug of alumina (2 in x ½ in). The solvent was removed under reduced pressure affording a yellow-brown solid. The solid was washed with cold pentane (3 x 15 ml) and was dried briefly under vacuum affording a yellow powder. Yield: 0.22 g (0.26 mmol, 41%). ^{1}H NMR (500 MHz, THF-d_8, 298 K): δ 7.32 (m, 2H, Ar*H*), 6.96 (m, 4H, Ar*H*), 3.62 (s, 4H, NCH_2Ar), 3.27 (m, 2H, PCH_2N), 3.18 (m, 2H, PCH_2N), 2.40 (m, 2H, PCH_2N), 2.27 (m, 2H, PCH_2N), 2.14 (m, 2H, PCH_2CH$_3$), 2.02 (m, 2H, PCH_2CH$_3$), 1.93 (m, 2H, PCH_2CH$_3$), 1.55 (m, 2H, PCH_2CH$_3$), 1.50 (m, 2H, PCH_2CH$_3$), 1.42 (m, 4H, PCH_2CH$_3$), 1.38 (m, 2H, PCH_2CH$_3$), 0.99 (m, 18H, PCH$_2$CH_3), 0.92 (m, 6H, PCH$_2$CH_3). ^{31}P{^{1}H} NMR (202.4 MHz, THF-d_8, 298 K): δ 16.1 (dd, 2P, $^{1}J_{PP}$ = 24.6 Hz), 12.8 (dd, 2P, $^{1}J_{PP}$ = 24.6 Hz). ^{19}F NMR (470.5 MHz, THF-d_8, 298 K): δ -116.5 (m, 4F). ^{15}N{^{1}H} NMR (50.7 MHz, THF-d_8, 298 K): δ -23.6 (d, 2N, Mo-N≡*N*, $^{1}J_{NN}$ = 6 Hz), -39.1 (m, 2N, Mo-*N*≡N). IR (THF): ν_{NN} cm^{-1} = 2012, 1950. Anal. Calcd. for $C_{34}H_{58}MoF_4N_6P_4$: C, 48.2; H, 6.9; N, 9.9. Found: C, 48.8; H, 7.1; N, 8.75. Complex **2** has a short lifetime in THF at 40 °C and readily isomerizes to the trans isomer upon heating over several hours.

cis-[W(N$_2$)$_2$(P^{Et}N$^{2,6\text{-F2-Bn}}$P^{Et})$_2$] (**3**): WCl$_4$(PPh$_3$)$_2$ (0.37 g, 0.43 mmol) was added to a stirring THF (50 mL) solution of P^{Et}N$^{2,6\text{-F2-Bn}}$P^{Et} (0.30 g, 0.86 mmol). Magnesium (1g, 41 mmol) was added and the reaction was stirred for 24 h turning orange. The reaction was filtered through a plug of alumina (2 in x ½ in). The solution was reduced to 7 mL and 50 mL of pentane was added to precipitate a beige powder. The powder was filtered off. The remaining orange-yellow solution was reduced to 3 mL under vacuum and layered with pentane and placed in a -35 °C freezer. A

yellow solid precipitated over 16 h that was collected and washed with pentane. The solid was dried briefly under vacuum affording a yellow powder. Yield: 0.25 g (0.27 mmol, 62%). ^{1}H NMR (500 MHz, THF-d_8, 298 K): δ 7.32 (m, 2H, Ar*H*), 6.97 (m, 4H, Ar*H*), 3.60 (s, 4H, NCH_2Ar), 3.37 (m, 2H, PCH_2N), 3.31 (m, 2H, PCH_2N), 2.41 (m, 2H, PCH_2N), 2.29 (m, 4H, PCH_2N), 2.24 (m, 2H, PCH_2CH$_3$), 2.15 (m, 2H, PCH_2CH$_3$), 2.05 (m, 2H, PCH_2CH$_3$), 1.64 (m, 4H, PCH_2CH$_3$), 1.50 (m, 4H, PCH_2CH$_3$), 1.39 (m, 2H, PCH_2CH$_3$), 0.97 (m, 18H, PCH$_2$CH_3), 0.90 (m, 6H, PCH$_2$CH_3). ^{13}C{^{1}H} NMR (125.7 MHz, THF-d_8, 298 K): δ 163.3 (m, Ar*C*F, $^{1}J_{CF}$ = 247 Hz), 130.6 (m, Ar*C*, $^{1}J_{CF}$ = 165 Hz, $^{3}J_{CF}$ = 11 Hz), 114.9 (s, Ar*C*), 112.0 (m, Ar*C*, $^{1}J_{CF}$ = 166 Hz), 59.4 (m, N*C*H$_2$P), 55.4 (m, N*C*H$_2$Ar), 29.9 (m, P*C*H$_2$CH$_3$), 18.2-23.6 (m, P*C*H$_2$CH$_3$) 6.2-11.6 (m, PCH$_2$*C*H$_3$). ^{31}P{^{1}H} NMR (202.4 MHz, THF-d_8, 298 K): δ -12.1 (dd, 2P, $^{1}J_{PP}$ = 14.9 Hz, $^{1}J_{183WP}$ = 297 Hz), -14.5 (dd, 2P, $^{1}J_{PP}$ = 14.9 Hz, $^{1}J_{183WP}$ = 303 Hz). ^{19}F NMR (470.5 MHz, THF-d_8, 298 K): δ -116.4 (m, 4F). ^{15}N{^{1}H} NMR (50.7 MHz, THF-d_8, 298 K): δ -24.9 (d, 2N, W-N≡*N*, $^{1}J_{NN}$ = 6 Hz), -60.4 (m, 2N, W-*N*≡N). IR (THF): ν_{NN} cm^{-1} = 1987, 1925. Anal. Calcd. for $C_{34}H_{58}WF_4N_6P_4$: C, 43.7; H, 6.3; N, 9.0. Found: C, 43.9; H, 6.3; N, 8.8. Complex **3** is remarkably stable in THF at 40 °C, and after 5 days only ~30% of **3** has isomerized to the trans isomer, a singlet at -16.5 ppm with ^{183}W sidebands ($^{1}J_{183WP}$ = 301 Hz) in the ^{31}P NMR spectrum.

Protonolysis Procedure for 1-3

In a typical experiment, a known amount of complex **1-3**, (*cis*-[M(N$_2$)$_2$(P^{Et}N$^{2,6\text{-F-Bn}}$P^{Et})$_2$]) (ca. 3-12 mmol) and 1,3,5-trimethoxybenzene was weighed into a rubber septum capped NMR tube and dissolved in THF-d_8. The solution was cooled to -40 °C in the NMR probe. Once the solution had temperature equilibrated for several minutes the tube was ejected and excess triflic acid (50-100 eq.) was added by microliter syringe to the cooled sample. The contents of the reaction were mixed by inversion of the NMR tube, and the sample was quickly returned to the

cold NMR probe. The sample was allowed to equilibrate to the temperature of the -40 °C NMR probe before initiating data collection. Room temperatures experiments were performed using an identical procedure with an NMR probe maintained at 25 °C.

Quantification of $N_2H_5^+$ and NH_4^+ by ^1H NMR spectroscopy.

To accurately quantify $N_2H_5^+$ (broad singlet at 10.8 ppm) and NH_4^+ (1:1:1 triplet, 7.0 ppm, J_{NH} = 51 Hz) formed in the protonolysis studies with HOTf, these product resonances were integrated versus 1,3,5-trimethoxybenzene resonances at 6.03 ppm. ^1H NMR spectra were collected using a 5 or 10 s delay time between scans to ensure complete relaxation of the sample for accurate integration. Manual peak integration of the ^1H NMR spectra was carried out after performing a full spectrum baseline correction. Due to the overlap of NH_4^+ resonances with aromatic resonances of the PNP ligand, the NH_4^+ resonances and the $N_2H_5^+$ resonance were also analyzed by peak shape analysis to compare to the values obtained my manual peak integration. Peak fitting of the ^1H NMR resonances for $N_2H_5^+$ and NH_4^+ was preformed using the CRAFT (**C**omplete **R**eduction to **A**mplitude **F**requency **T**able) analysis software package included in the VNMRJ 4.2 software suite.[4] Processing parameters include 0.2 Hz line broadening with maximum line widths defined in CRAFT as 35 Hz. Signal amplitudes were determined relative to the internal standard of the aromatic protons of 1,3,5-trimethoxybenzene at 6.03 ppm. Tabulated results for protonolysis studies of complexes **1**, **2**, and **3** are listed in Table S3. CRAFT simulated ^1H NMR data are shown in Fig. S7.

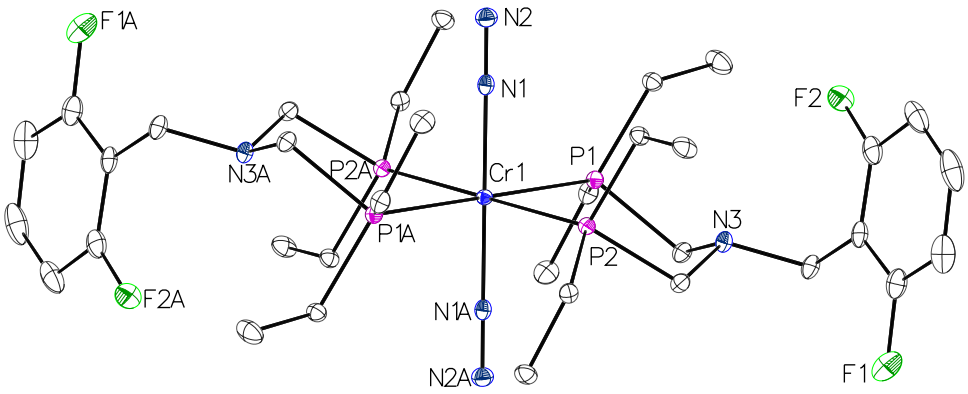

Fig. S1. Molecular structure of *trans*-[$Cr(N_2)_2(P^{Et}N^{2,6\text{-}F2\text{-}Bn}P^{Et})_2$] (*trans*-**1**). Thermal ellipsoids are drawn at 50% probability. Hydrogen atoms are omitted for clarity. Selected bond distances (Å): (**1**) Cr–P1 = 2.3546(4); Cr–P2 = 2.3535(4); Cr–N1 = 1.8858(14); N1–N2 = 1.1274(19).

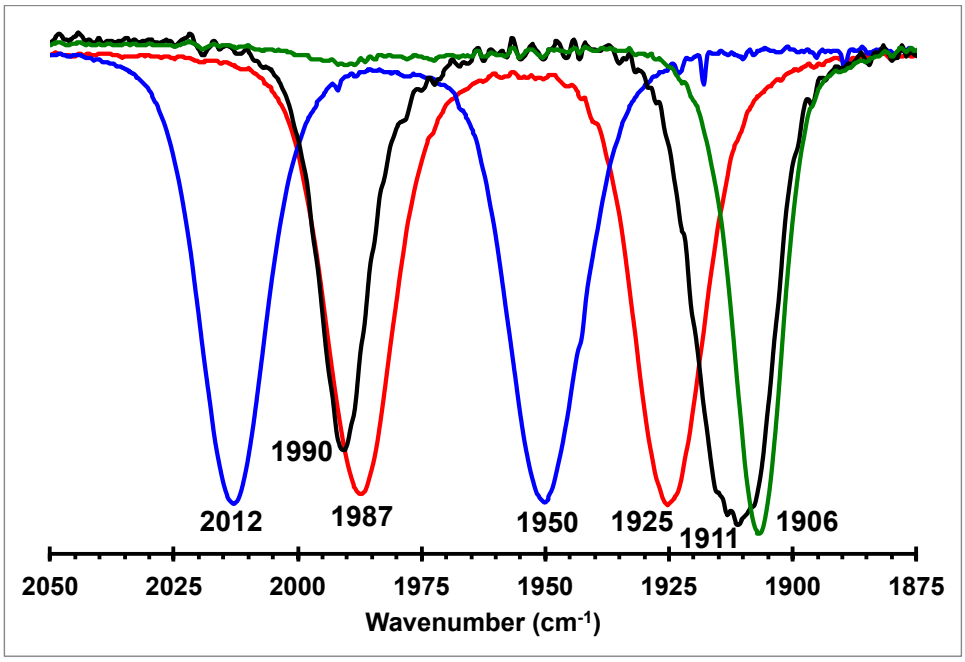

Fig. S2. FTIR spectra collected in THF showing the $^{14}N_2$ bands of *trans*-[$Cr(N_2)_2(P^{Et}N^{2,6\text{-}F2\text{-}Bn}P^{Et})_2$] (*trans*-**1**; green), *cis*-[$Cr(N_2)_2(P^{Et}N^{2,6\text{-}F2\text{-}Bn}P^{Et})_2$] (**1**; black), *cis*-[$Mo(N_2)_2(P^{Et}N^{2,6\text{-}F2\text{-}Bn}P^{Et})_2$] (**2**; blue), *cis*-[$W(N_2)_2(P^{Et}N^{2,6\text{-}F2\text{-}Bn}P^{Et})_2$] (**3**; red).

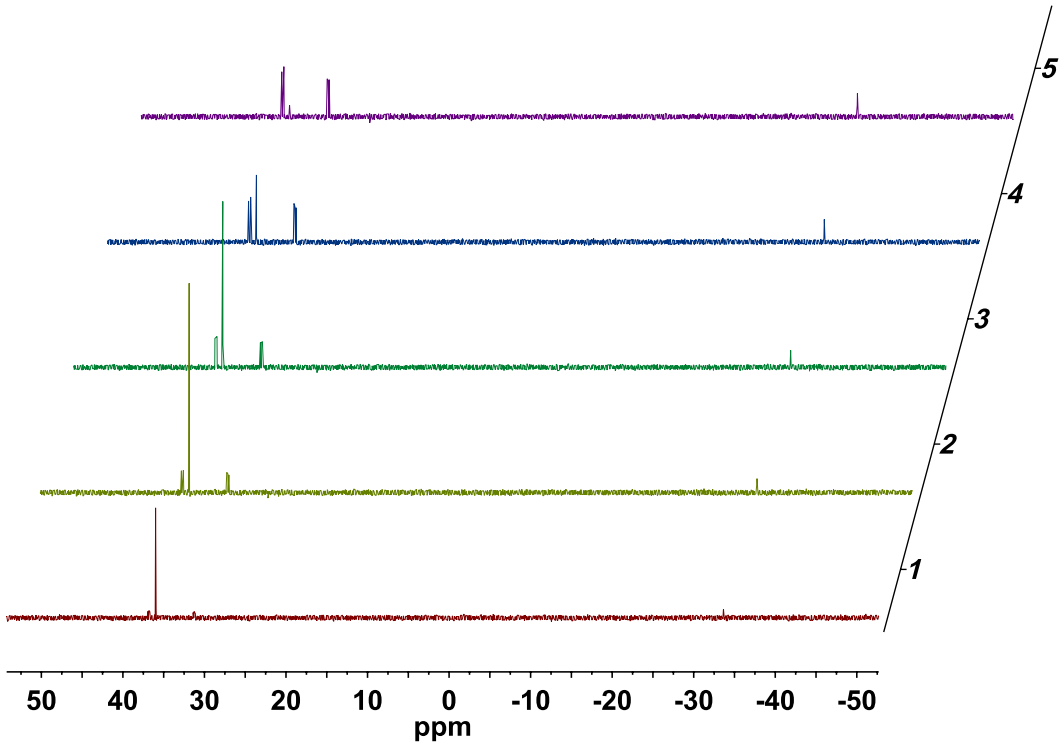

Fig. S3. ^{31}P NMR spectra collected in THF at 25 °C showing the isomerization of *trans*-[$Cr(N_2)_2(P^{Et}N^{2,6\text{-}F2\text{-}Bn}P^{Et})_2$] (*trans*-**1**) to *cis*-[$Cr(N_2)_2(P^{Et}N^{2,6\text{-}F2\text{-}Bn}P^{Et})_2$] (**1**). Trace 1: Initial ^{31}P spectrum; Trace 2: after 1 h; Trace 3: after 2.5 h; Trace 4: after 4.5 h; Trace 5: after 21.5 h. The resonance at 33.6 ppm is free $P^{Et}N^{2,6\text{-}F2\text{-}Bn}P^{Et}$ ligand.

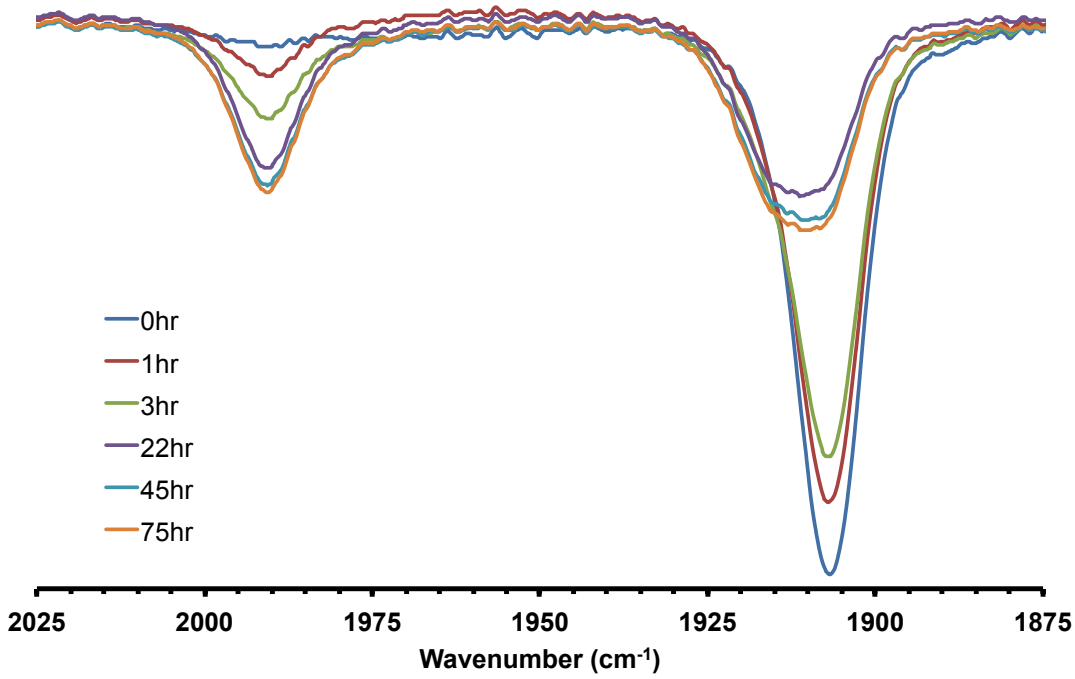

Fig. S4. FTIR spectra collected in THF at room temperature showing the isomerization of *trans*-[$Cr(N_2)_2(P^{Et}N^{2,6\text{-}F2\text{-}Bn}P^{Et})_2$] (*trans*-**1**) to *cis*-[$Cr(N_2)_2(P^{Et}N^{2,6\text{-}F2\text{-}Bn}P^{Et})_2$] (**1**) over 75 h.

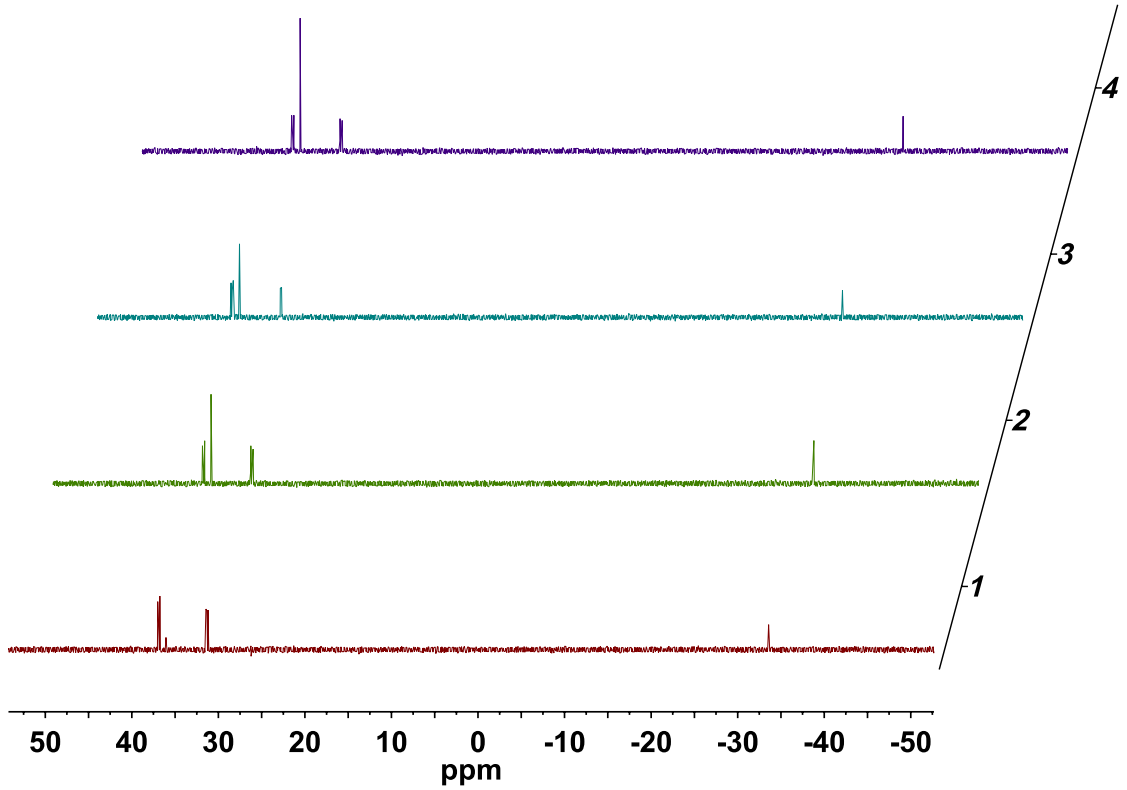

Fig. S5. ^{31}P NMR spectra collected in THF at 25 °C showing the isomerization of *cis*-[Cr(N$_2$)$_2$(P^{Et}N$^{2,6\text{-F2-Bn}}$P^{Et})$_2$] (**1**) to *trans*-[Cr(N$_2$)$_2$(P^{Et}N$^{2,6\text{-F2-Bn}}$P^{Et})$_2$] (*trans*-**1**) after prolonged heating of the sample at 40 °C. Trace 1: Initial ^{31}P spectrum; Trace 2: after 1 day at 40 °C; Trace 3: after 2 days at 40 °C; Trace 4: after 3 days at 40 °C. The resonance at 33.6 ppm is free P^{Et}N$^{2,6\text{-F2-Bn}}$P^{Et} ligand.

Table S1. Determination of N-N force constants for **1**, **2**, and **3**. The method and equations to obtain the values of k and k_c is described in *J. Am. Chem. Soc.* **1962**, 84, 4432-4438.

	ν_1	ν_2	μ	λ_1	λ_2	k (mdynes/Å)	k_c (mdynes/Å)
Cr	1990	1911	0.1428	233210.2	215061.6	15.69	0.64
Mo	2012	1950	0.1428	238395.2	223929.2	16.18	0.51
W	1987	1925	0.1428	232507.6	218224.2	15.78	0.50

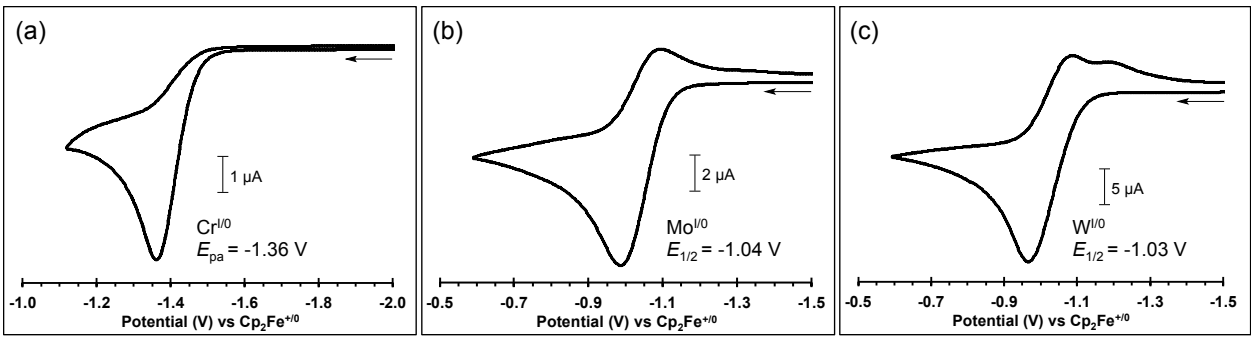

Fig. S6 Cyclic voltammograms of (a) **1**; (b) **2**; (c) **3** recorded at υ = 0.10 V s^{-1}. Conditions: 0.2 M $[Bu_4N][B(C_6F_5)_4]$ THF solution, glassy carbon working electrode, 25 °C, 0.6 mM **1**; 0.9 mM **2**; 1.4 mM **3**.

Kinetic analysis of the irreversible $Cr^{I/0}$ wave in the cyclic voltammetry experiment

Assuming the $Cr^{I/0}$ couple of **1** is irreversible due to rapid loss of N_2 from the oxidized species, the oxidation wave can be analyzed according to an electrochemical E_rC_i mechanism (a reversible electron transfer followed by an irreversible chemical reaction). The oxidation wave of **1** is irreversible at all scan rates examined (0.1 to 20 V s^{-1}), indicating that the wave is controlled by the kinetics of the chemical step according to Equation S1.1:

$$E_{pa} = E^{\circ'} + 0.78\frac{RT}{F} - 1.15\frac{RT}{F}\log\left(\frac{RTk}{F\,\upsilon}\right) \qquad (eq.S1.1)$$

where E_{pa} is the anodic peak potential (V), $E^{\circ\prime}$ is the formal potential of the $Cr^{I/0}$ couple (V), F is the Faraday constant, R is the gas constant, T is the temperature (K), υ is the scan rate (V s^{-1}), and k is the first-order rate constant (s^{-1}) for N_2 dissociation from Cr^I.[5,6] This equation cannot be solved accurately for **1** since two of the variables ($E^{\circ\prime}$ and k) are unknown. However, an upper limit on $E^{\circ\prime}$ can be estimated by assuming values of k. To this purpose, the value of E_{pa} = −1.36 V at υ = 0.1 V s^{-1} was used to generate estimated values of $E^{\circ\prime}$ for a range of k values (Table S2).

Note that the experimental E_{pa} value is also affected by iR drop resulting from uncompensated resistance of the 0.2 M $[Bu_4N][B(C_6F_5)_4]$ THF electrolyte solution. In our

experiments, the $Cp_2Fe^{+/0}$ and $Cp^*_2Fe^{+/0}$ couples displayed a peak-to-peak separation (E_{pa}– E_{pc}) of ~130 mV, which is much larger than the value expected for an ideal Nernstian wave (57 mV at 25 °C), as well as the values we typically observe for the $Cp_2Fe^{+/0}$ wave in acetonitrile solvent at similar scan rates (65-70 mV). An estimate of the potential error due to *i*R drop can be made by taking the difference in E_{pa}– E_{pc} of the $Cp_2Fe^{+/0}$ couple in THF and acetonitrile and dividing by two. This conservative estimate suggests a corrected E_{pa} value of **1** is 30 mV more negative than observed, i.e. $E_{pa} = -1.39$ V at $\upsilon = 0.1$ V s^{-1}. Similarly, consideration of *i*R drop also results in the estimated $E^{\circ\prime}$ values in Table S2 being more negative by 30 mV, e.g. $E^{\circ\prime} = -1.12$ V when $k = 1 \times 10^9$ s^{-1}.

Table S2. Estimated Values of $E^{\circ\prime}$ for **1**.[a]

k (s^{-1})	$E^{\circ\prime}$ (V)
1×10^3	–1.27
1×10^4	–1.24
1×10^5	–1.21
1×10^6	–1.18
1×10^7	–1.15
1×10^8	–1.12
1×10^9	–1.09

[a] Calculated according to Equation S1.1 using $E_{pa} = -1.36$ V (uncorrected for *iR*-drop) and $\upsilon = 0.1$ V s^{-1}.

Table S3. Tabulated Results for protonolysis studies of complexes **1**, *trans*-**1**, **2**, **3**

	Metal (M)	(M) mass (mg)	Acid	Acid equiv	Temp °C	equiv NH_4^+ per M atom		equiv $NH_2NH_3^+$ per M atom	
						CRAFT	manual integration	CRAFT	manual integration
1	Cr (**1**)	2.7	HOTf	100	-40	0.13	0.13	0.28	0.34
2	Cr (**1**)	4.9	HOTf	100	-40	0.10	0.12	0.28	0.29
3	Cr (**1**)	2.0	HOTf	100	-40	0.06	0.11	0.19	0.20
4	Cr (**1**)	7.3	HOTf	100	-40	0.05	0.09	0.18	0.18
5	Cr (**1**)	3.6	HOTf	100	-40	0.06	0.12	0.20	0.20
6	Cr (**1**)	3.6	HOTf	100	RT	0	0	0	0
7	Cr (*trans*-**1**)	3.3	HOTf	100	-40	0.10	0.07	0.19	0.22
8	Cr (**1**)	1.0	H_2SO_4	100	RT	0	0	0	0
9	Mo (**2**)	11	HOTf	100	-40	0	0	0	0
10	Mo (**2**)	7.4	HOTf	100	RT	0	0	0	0
11	Mo (**2**)	5.3	H_2SO_4	100	RT	0	0	0	0
12	W (**3**)	2.9	HOTf	100	-40	0	0	0	0
13	W (**3**)	12.1	H_2SO_4	100	RT	0	0	0	0
14	W (**3**)	15.4	HOTf	35	-40	0	0	0	0
15	W (**3**)	8.7	HOTf	61	-40	0	0	0	0

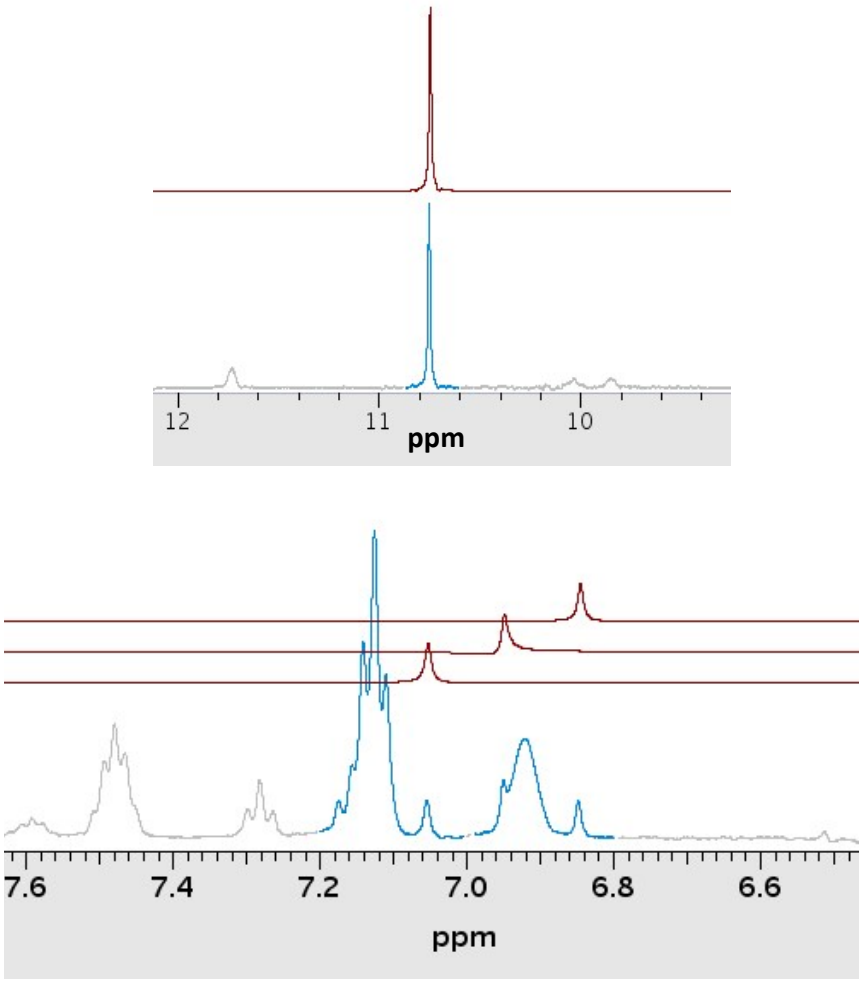

Fig. S7. Measured ^{1}H NMR data (blue) and simulated CRAFT ^{1}H NMR data (red) of the resonances for $N_2H_5^+$ (top spectrum) and NH_4^+ (bottom spectrum).

General procedure for X-ray diffraction studies: Single crystals were selected and mounted using NVH immersion oil onto a glass fiber, a nylon fiber and cooled to the data collection temperature of 100(2) K with a stream of dry nitrogen gas. Data were collected on a Brüker-AXS Kappa APEX II CCD diffractometer with 0.71073 Å Mo-Kα radiation. Unit cell parameters were obtained from 60 data frames, 0.5º ϕ, from three different sections of the Ewald sphere and complete data collection strategies were determined for each crystal using the APEX2 suite.[7] Each data set was treated with SADABS absorption corrections based on redundant multi-scan data.[8] The structures were solved by direct methods (XS) or intrinsic phasing (XT) and refined by least squares method on F^2 using the XL program package interfaced through OLEX2.[9-11] All non-hydrogen atoms were refined with anisotropic displacement parameters and all hydrogen atoms were treated as idealized contributions, unless otherwise noted. Details regarding specific solution refinement for each compound are provided below.

Refinement of **1**: Data were collected on a yellow prism (0.25 x 0.20 x 0.06 mm^3) grown by evaporation of a diethyl ether solution. The data set consisting of 92748 reflections (11730 unique, R_{int} = 7.03%) was collected over 2θ = 2.928 to 60.068°. The metric symmetry and systematic absences were consistent with the monoclinic space group $P2_1/n$. The asymmetric unit contains one molecule of *cis*-$[Cr(N_2)_2(P^{Et}N^{2,6\text{-}F2\text{-}Bn}P^{Et})_2]$ that is bisected by a non-crystallographic pseudo-2-fold axis parallel to the crystallographic *b* axis. The goodness of fit on F^2 was 1.027 with R_1 = 3.87% [I>2σ(I)], wR_2 = 9.69% (all data) and with a largest difference peak and hole of 0.50 and –0.38 e/Å^3.

Refinement of *trans*-**1**: Data were collected on an orange block (0.15 x 0.15 x 0.06 mm^3) grown by rapid evaporation of a diethyl ether solution. The data set consisting of 48915 reflections (5435 unique, R_{int} = 7.00%) was collected over 2θ = 3.812 to 59.148°. The metric symmetry and systematic absences were consistent with the monoclinic space group $P2_1/c$. The asymmetric unit contains one molecule of *trans*-$[Cr(N_2)_2(P^{Et}N^{2,6\text{-}F2\text{-}Bn}P^{Et})_2]$. The goodness of fit on F^2 was 1.024with R_1 = 3.44% [I>2σ (I)], wR_2 = 8.30% (all data) and with a largest difference peak and hole of 0.37 and –0.35 e/Å^3.

Refinement of **2**: Data were collected on a yellow shard (0.15 x 0.10 x 0.08 mm^3) grown by evaporation of a diethyl ether solution. The data set consisting of 68516 reflections (19824 unique, R_{int} = 8.37%) was collected over 2θ = 2.92 to 56.566°. The metric symmetry and systematic absences were consistent with the monoclinic space group P*n*. The asymmetric unit contains two molecules of *cis*-[$Mo(N_2)_2(P^{Et}N^{2,6\text{-}F2\text{-}Bn}P^{Et})_2$], which are nearly related by translation along the crystallographic *b* axis, but differ in the orientation of an ethyl group. A non-zero-Flack parameter indicated racemic twinning, and the data were treated as such with a freely refined twin ratio converging on ~78:22. The goodness of fit on F^2 was 1.003 with R_1 = 5.28% [$I>2\sigma(I)$], wR_2 = 10.71% (all data) and with a largest difference peak and hole of 1.03 and –0.44 $e/Å^3$. The largest residuals are near the heavy Mo atoms.

Refinement of **3**: Data were collected on a yellow block (0.23 x 0.22 x 0.15 mm^3) grown by evaporation of a diethyl ether solution. The data set consisting of 206157 reflections (39026 unique, R_{int} = 5.03%) was collected over 2θ = 2.922 to 72.636°. The metric symmetry and systematic absences were consistent with the monoclinic space group P*n*. The asymmetric unit contains two molecules of *cis*-[$W(N_2)_2(P^{Et}N^{2,6\text{-}F2\text{-}Bn}P^{Et})_2$], which are nearly related by translation along the crystallographic *b* axis, but differ in the orientation of an ethyl group. A non-zero-Flack parameter indicated racemic twinning, and the data were treated as such with a freely refined twin ratio converging on ~52:48. The goodness of fit on F^2 was 1.043 with R_1 = 3.12% [$I>2\sigma(I)$], wR_2 = 6.30% (all data) and with a largest difference peak and hole of 5.08 and –1.28 $e/Å^3$. The large residuals are near the heavy W atoms.

Table S4. Crystallographic data for complexes **1**, *trans*-**1**, and **2**.

	1	*trans*-**1**	**2**
Formula	$C_{34}H_{58}CrF_4N_6P_4$	$C_{34}H_{58}CrF_4N_6P_4$	$C_{34}H_{58}MoF_4N_6P_4$
Crystal System	Monoclinic	Monoclinic	Monoclinic
Space Group	$P2_1/n$	$P2_1/c$	Pn
a, Å	10.3010(2)	10.8985(6)	10.2417(2)
b, Å	18.8047(4)	13.4410(7)	18.3288(3)
c, Å	20.7192(4)	13.4741(7)	21.5881(4)
α, deg	90	90	90
β, deg	93.7700(10)	101.392(3)	95.3341(11)
γ, deg	90	90	90
V, Å^3	4004.77(14)	1934.89(18)	4034.93(13)
Z	4	2	4
Radiation (λ, Å)	Mo-Kα, 0.71073	Mo-Kα, 0.71073	Mo-Kα, 0.71073
ρ (calcd.), g/cm^3	1.331	1.378	1.394
μ, mm^{-1}	0.496	0.514	0.534
Temp, K	100.0	100.0	100.0
Size, mm^3	0.25 x 0.2 x 0.06	0.15 x 0.15 x 0.06	0.15 x 0.1 x 0.08
Color	Yellow	Orange	Yellow
Habit	Prism	Block	Irregular
No. Reflections	92748	48915	68516
No. Ind. Ref. (R_{int})	11730 (0.0703)	5435 (0.0700)	19824 (0.0837)
2θ range, deg	2.928 - 60.068	3.812 - 59.148	2.92 – 56.566
R_1	0.0387	0.0344	0.0528
wR_2	0.0859	0.0743	0.0908
GOF (F^2)	1.027	1.024	1.003
F(000)	1696.0	848.0	1768.0

Table S5. Crystallographic data for complex **3**.

	3
Formula	$C_{34}H_{58}WF_4N_6P_4$
Crystal System	Monoclinic
Space Group	*Pn*
a, Å	10.2469(2)
b, Å	18.3292(3)
c, Å	21.5498(4)
α, deg	90
β, deg	95.4260(10)
γ, deg	90
V, Å^3	4029.29(13)
Z	4
Radiation (λ, Å)	Mo-Kα, 0.71073
ρ (calcd.), g/cm^3	1.541
μ, mm^{-1}	3.077
Temp, K	100
Size, mm^3	0.23 x 0.22 x 0.15
Color	Yellow
Habit	Block
No. Reflections	206157
No. Ind. Ref. (R_{int})	39026 (0.0503)
2θ range, deg	2.922 - 72.636
R_1	0.0312
wR_2	0.0601
GOF (F^2)	1.043
F(000)	1896.0

References for ESI.

1. C. J. Weiss, A. N. Groves, M. T. Mock, W. G. Dougherty, W. S. Kassel, M. L. Helm, D. L. DuBois and R. M. Bullock, Dalton Trans., 2012, 41, 4517-4529.

2. J. R. Dilworth and R. L. Richards, Inorg. Synth., 2007, 20, 33-43.

3. L. A. Labios, C. J. Weiss, J. D. Egbert, S. Lense, R. M. Bullock, W. G. Dougherty, W. S. Kassel and M. T. Mock, Z. Anorg. Allg. Chem., 2015, 641, 105-117.

4. K. Krishnamurthy, Magn. Reson. Chem., 2013, 51, 821-829.

5. Bard, A. J.; Faulkner, L. R. Electrochemical Methods: Fundamentals and Applications; 2nd ed.; John Wiley & Sons: Hoboken, NJ, 2001.

6. Savéant, J. M. Elements of Molecular and Biomolecular Electrochemistry: An Electrochemical Approach to Election Transfer Chemistry; Wiley, 2006.

7. APEX2. Bruker AXS Inc., Madison, Wisconsin, USA.

8. SADABS-2014/5. Bruker AXS Inc., Madison, Wisconsin, USA.

9. Sheldrick, G.M. (2015). Acta Cryst. A71, 3-8.

10. Sheldrick, G.M. (2008). Acta Cryst. A64, 112-122.

11. Dolomanov, O.V., Bourhis, L.J., Gildea, R.J, Howard, J.A.K. & Puschmann, H. (2009), J. Appl. Cryst. 42, 339-341.

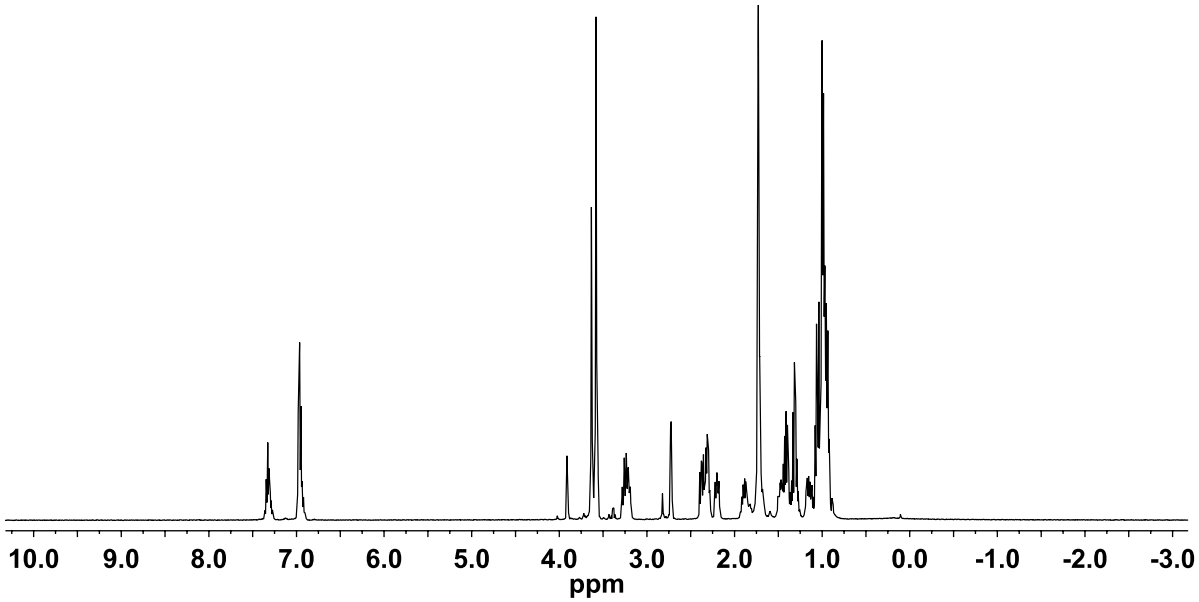

Fig. S8. ^{1}H NMR spectrum of **1** recorded in THF-d_8.

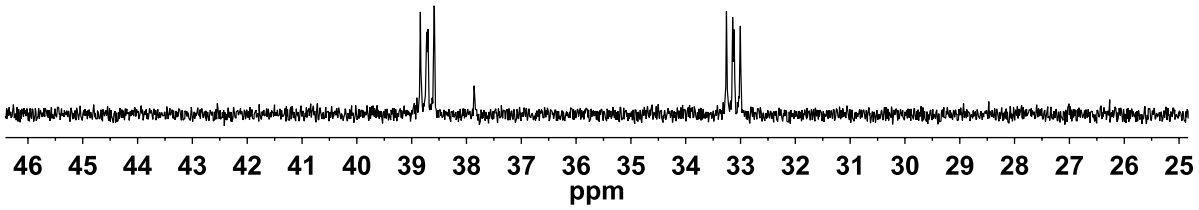

Fig. S9. ^{31}P{^{1}H} NMR spectrum of **1** recorded in THF-d_8.

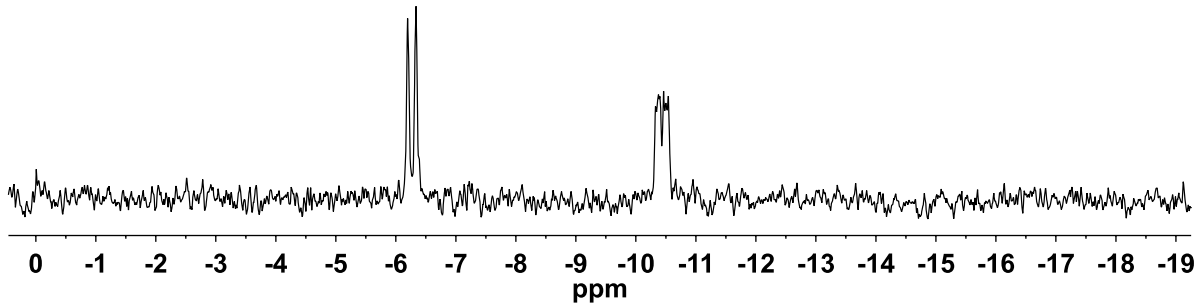

Fig. S10. $^{15}N\{^{1}H\}$ NMR spectrum of $\mathbf{1^{15N}}$ recorded in THF-d_8.

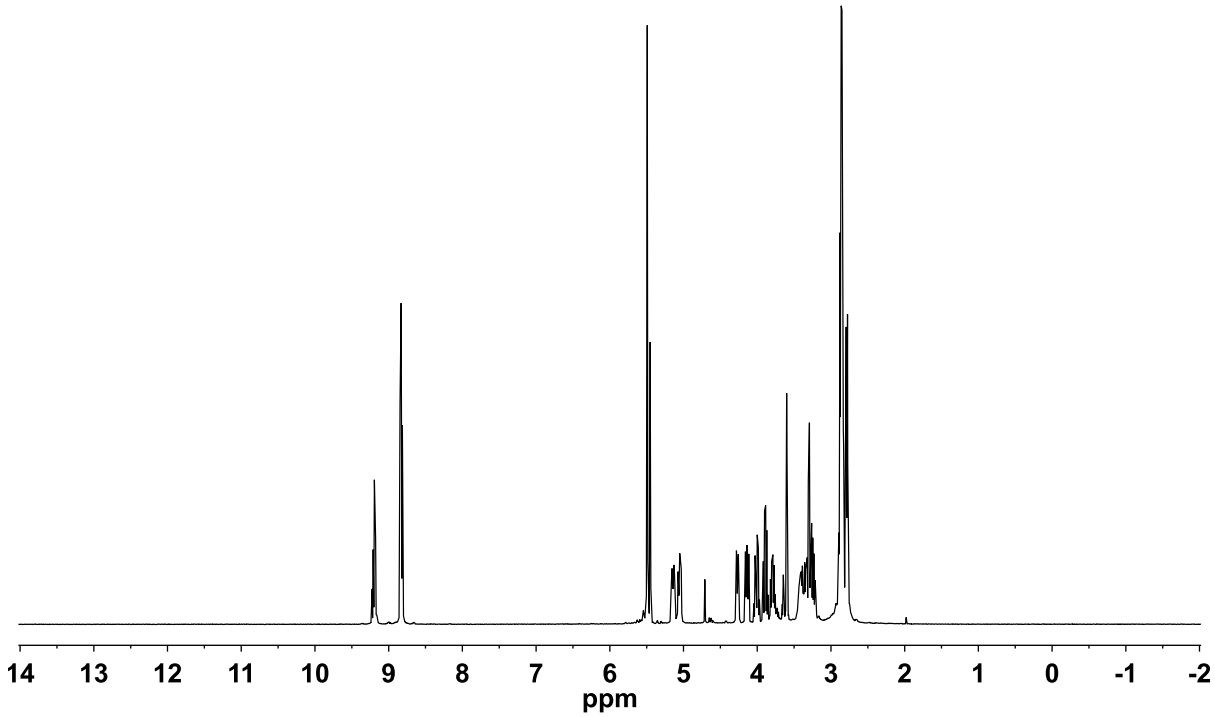

Fig. S11. ^{1}H NMR spectrum of **2** recorded in THF-d_8.

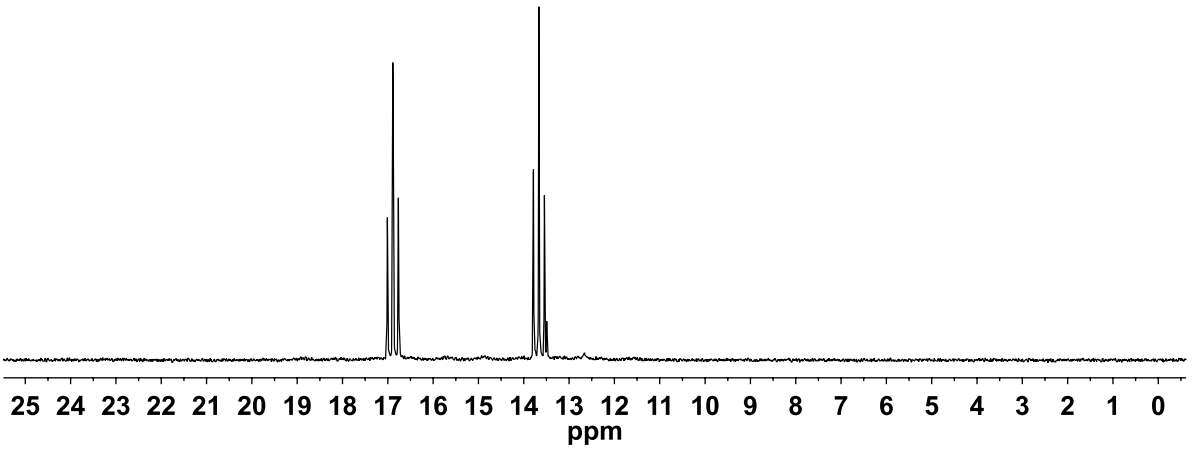

Fig. S12. $^{31}P\{^{1}H\}$ NMR spectrum of **2** recorded in THF-d_8.

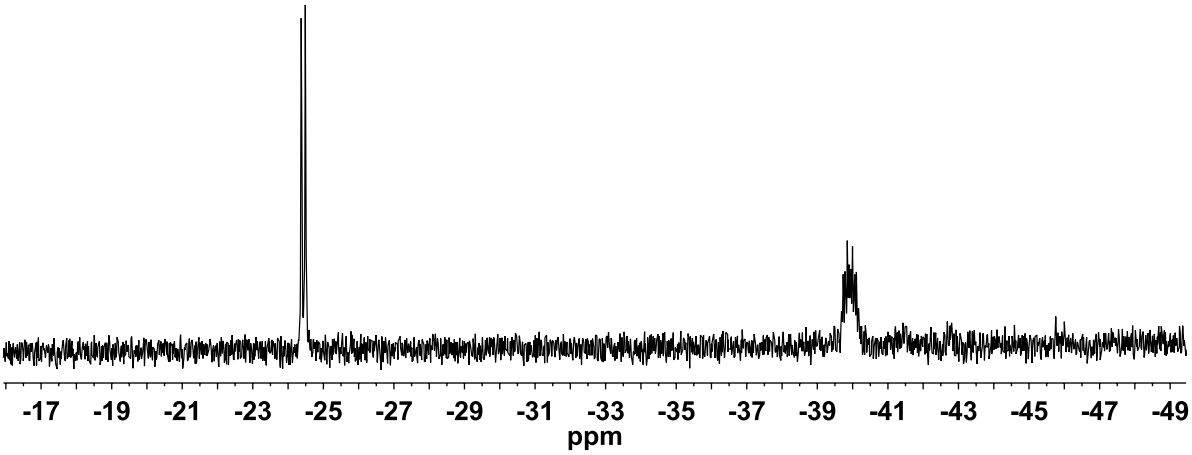

Fig. S13. $^{15}N\{^{1}H\}$ NMR spectrum of $\mathbf{2^{15N}}$ recorded in THF-d_8.

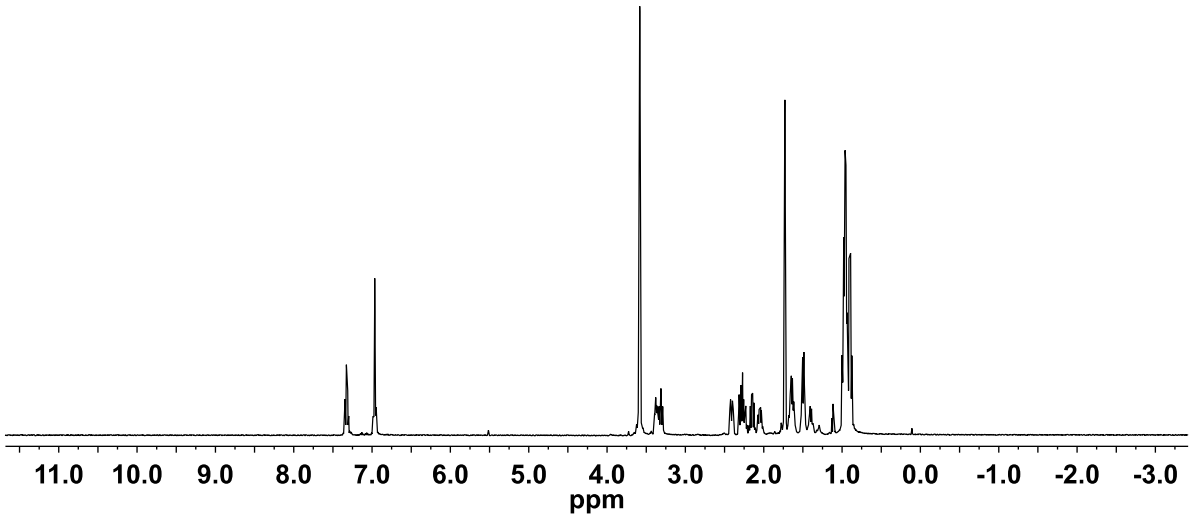

Fig. S14. ^{1}H NMR spectrum of **3** recorded in THF-d_8.

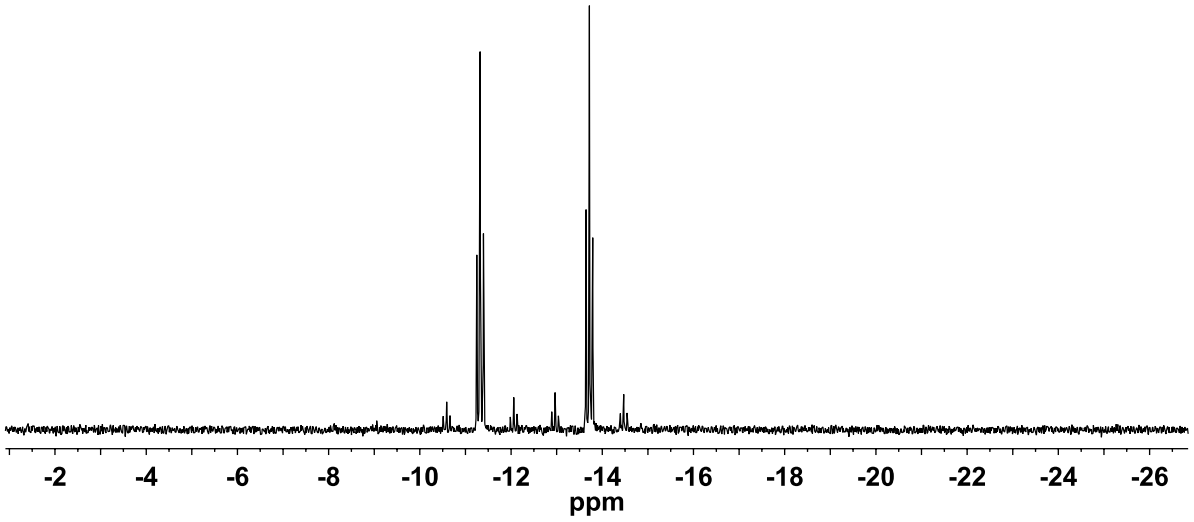

Fig. S15. ^{31}P{^{1}H} NMR spectrum of **3** recorded in THF-d_8.

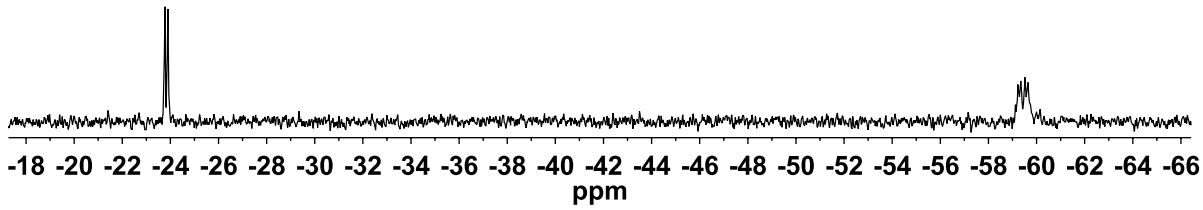

Fig. S16. $^{15}N\{^{1}H\}$ NMR spectrum of $\mathbf{3^{15N}}$ recorded in THF-d_8.

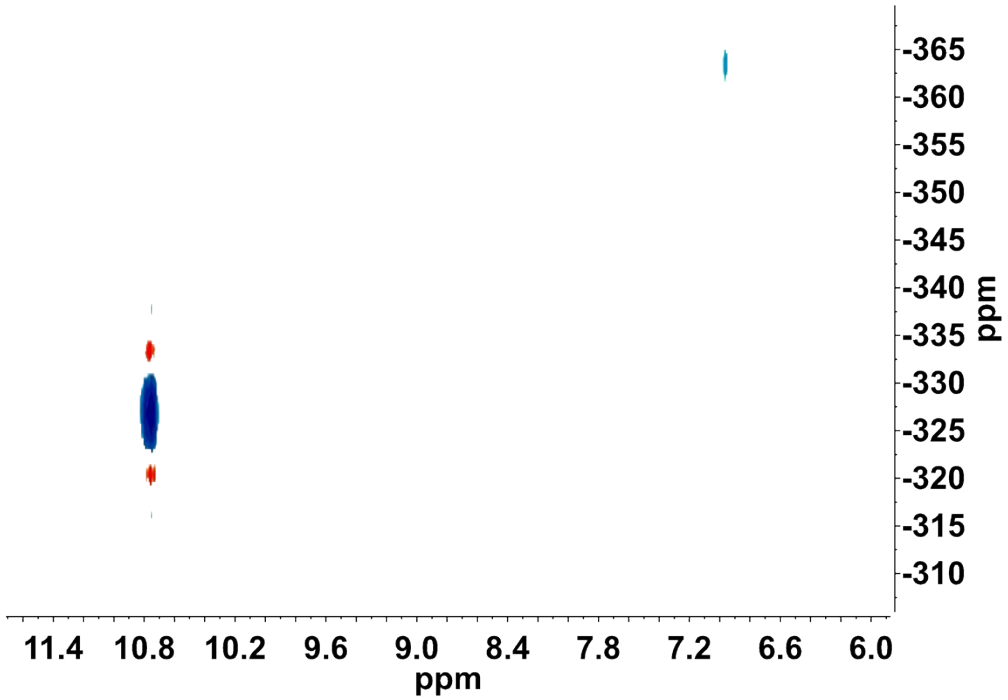

Fig. S17. ^{1}H-^{15}N HSQC NMR spectrum recorded in THF-d_8 at -40 °C from the addition of HOTf to *cis*-[Cr($^{15}N_2$)$_2$($P^{Et}N^{2,6\text{-}F2\text{-}Bn}P^{Et}$)$_2$] ($\mathbf{1^{15N}}$). The cross-peak 10.8/-326 corresponds to $^{15}N_2H_5^+$. The cross-peak 7.0/-364 corresponds to $^{15}NH_4^+$.

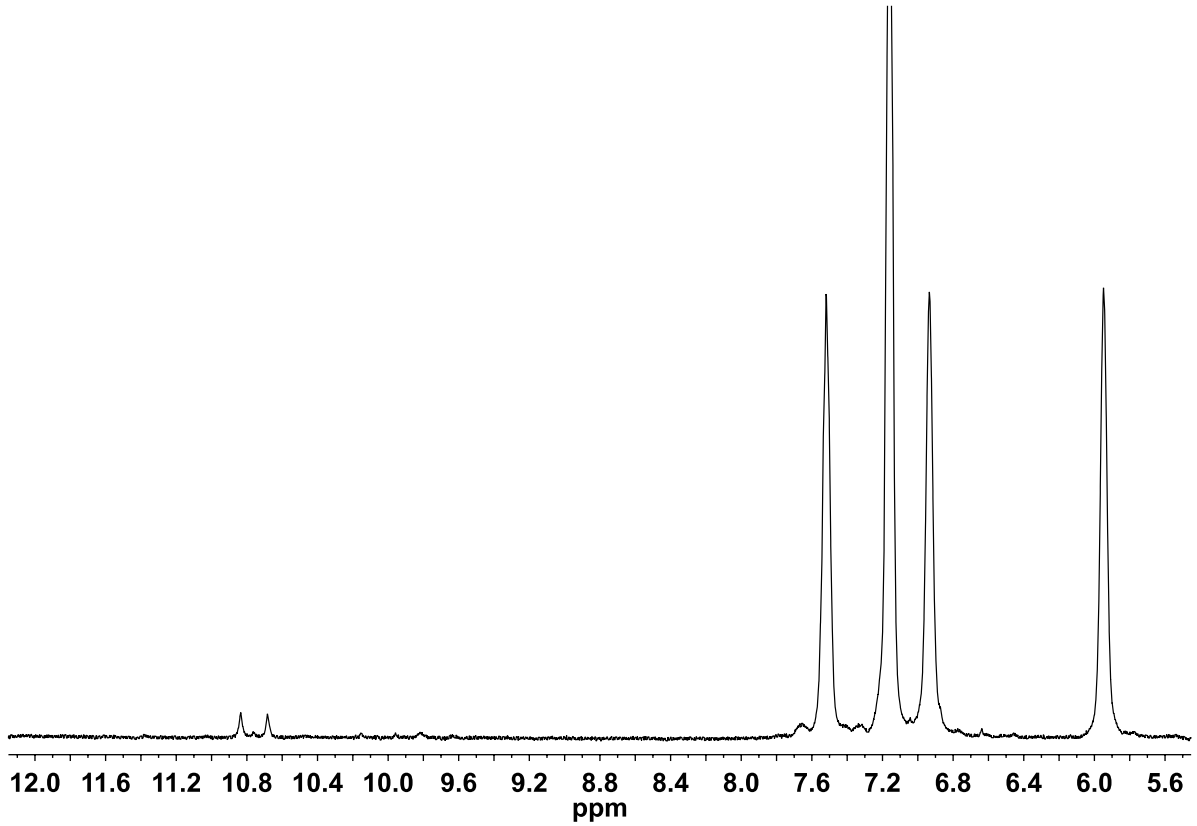

Fig. S18. ^{1}H NMR spectrum recorded in THF-d_8 at -40 °C from the addition of HOTf to *cis*-[Cr(^{15}N$_2$)$_2$(P^{Et}N$^{2,6\text{-F2-Bn}}$P^{Et})$_2$] (**1^{15N}**), showing the doublet for $^{15}N_2H_5^+$ (J_{NH} = 75 Hz). The doublet for $^{15}NH_4^+$ at 7.0 ppm is obscured by aromatic resonances of PNP ligand.

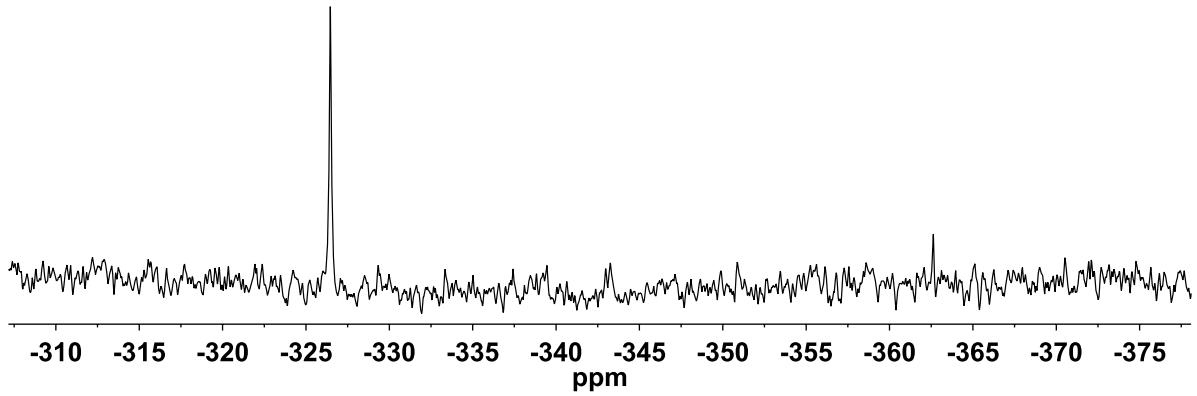

Fig. S19. $^{15}N\{^{1}H\}$ NMR spectrum recorded in THF-d_8 at -40 °C from the addition of HOTf to *cis*-[Cr($^{15}N_2$)$_2$($P^{Et}N^{2,6\text{-}F2\text{-}Bn}P^{Et}$)$_2$] (**1^{15N}**), showing the singlet for $^{15}N_2H_5^+$ at -326 ppm. The singlet for $^{15}NH_4^+$ is at -364 ppm.